Theoretical Studies on Blue versus Red Shifts in Diglyme−M^+−X^- (M = Li, Na, and K and X = CF_3SO_3, PF_6, and $(CF_3SO_2)_2N$))

Nilesh R. Dhumal and Shridhar P. Gejji*

Department of Chemsitry, University of Pune, Pune - 411007, India

Received: July 29, 2005; In Final Form: October 29, 2005

Ab initio Hartree−Fock calculations have been used to obtain the electronic structure and the frequencies of normal vibrations in the 1:1:1 solid polymer electrolytes $CH_3(OCH_2CH_2)_2OCH_3$−M^+−X^- (M = Li, Na, and K and X = CF_3SO_3, PF_6, $(CF_3SO_2)_2N$). These calculations predict stronger binding for the lithium ion toward the ether oxygens of diglyme in these electrolytes. Consequences of diglyme−MX interactions to the infrared spectra have been presented. Natural bond analysis and the electron density topography have been used to explain the direction of the frequency shifts of the normal vibrations of the anions in these electrolytes.

1. Introduction

Poly(ethylene oxide) (PEO) oligomers complexed with organic and inorganic salts in solutions or solids[1] have been of considerable interest in the recent literature. Wright[2] has found the crystalline and amorphous PEO complexes of alkali metal salts and suggested their use as solid electrolytes or high ionic conductors.[3,4] These solid polymer electrolytes (SPE) are crucial in the development of modern high-energy density lithium secondary batteries. Most new types of solid polymer electrolytes rely on ethylene oxide unit, $(CH_2-CH_2-O)_n$, which coordinates with Li^+ and thereby dissolving it in the polymer matrix.[5] New lithium salts are economical, stable, and able to provide large number of fast moving charge carries to meet the demands on ion conductivity. Lithium salts based on weakly coordinating anions such as $CF_3SO_3^-$ (triflate or Tf^-), PF_6^-, and $(CF_3SO_2)_2N^-$ (TFSI), serve as good anions for SPE purposes.[6] These weakly coordinating anions render high ionic conductivity. Thus the anion−metal ion as well as PEO oligomer−metal ion interactions at the molecular level are important in understanding of ion transport phenomenon in these electrolytes.[7] Coordination of metal ion to ether oxygens of PEO oligomers which engenders polymer segmental motion govern a number of properties of these electrolytes.[8] With this view a number of theoretical studies aimed to characterize these ion−polymer and ion−ion interactions in PEO have appeared in the literature. Gejji et al.[8−10] have studied the 1:1 lithium−diglyme ion pairs with the Li^+ coordinated by two and three ether oxygens by employing the ab initio molecular orbital calculations. This work has been *extended* to 1:1 complexes of a Li^+ with tetra-, penta-, and hexaglymes in order to understand the role of cation oxygen atoms interactions in SPE.[11] Quantum chemical calculations including the electron correlation using the perturbation theory have been employed to derive electronic structure and vibrational frequencies of isolated Tf^- and Li^+-Tf^- ion pairs with the use of Gaussian basis sets.[12,13] Analysis of normal vibrations in the Li^+Tf^- ion pair conformers reveals a downshift of 38 cm^{-1} for the symmetric SO_3 stretching for the bidentate coordination of the metal ion relative to that in the isolated Tf^-; in contrast a frequency shift of 42 cm^{-1} in the opposite direction has been predicted for the monodentate complex. Measured infrared and Raman spectra of crystalline PEO oligomers complexed with LiTf and NaTf have shown a five-coordinated Li^+ acompanying a conformation change of the adjacent ethylene oxide sequence in SPE.[14,15] In PEO−NaTf SPE, the coordination number of metal ion varies from 5 to 7 for varying contributions from ether and anionic oxygens. It has been noticed that the increasing number of ethylene oxide units facilitates higher coordination number for the metal ion. Raman and IR spectra of NaTf and LiTf in these electrolytes display multiple bands for the SO_3 and CF_3 vibrations.[16,17] A comparison of the vibrational spectra of AgTf, NaTf, and NH_4-Tf $[Bu_4N]Tf$ ion pairs reveals that the SO_3 and the CF_3 vibrations are sensitive to the different potential-energy environments of the anion.[18] Thus cation−anion interactions cause variation from 1251 to 1285 cm^{-1} for the asymmetric SO_3 stretching vibration in these ion pairs, and a variation from 1149 cm^{-1} to 1188 cm^{-1} has been noticed for the corresponding CF_3 stretching. It should be remarked here that the triflate anion in [Bu4N}Tf^- ion pair has been described as a free anion with the underlying assumption being the bulky nature of the cation minizes cation−triflate interactions.[19] Absence of such interactions in quantum mechanically derived vibrational spectra of the "free anion" pose difficulties in a direct comparison with the wavenumbers of normal vibrations in the calculated spectra to the observed spectra for the free Tf^- anion. A suitable electrolyte for secondary lithium batteries can be obtained by dissolving the lithium−hexafluorophosphate ($LiPF_6$) in aprotic solvents.[20] Spectroscopic investigations of the IR active ν_3 and ν_4 modes of PF_6^- have shown that $Li^+PF_6^-$ ion pairs are favored in aprotic solvents and the nondegenerate symmetric stretching in the Raman and IR spectra of PF_6^- can be used as a probe to distinguish different ion pairs in the polymer electrolytes. The symmetric stretching (ν_1) vibration in the PF_6^- anion is only Raman active, and the perturbation of the symmetry on cation coordination, however, results in this vibration to be IR active. Studies on the single ion transport in crystalline $LiPF_6(PEO)_6$ have shown that the activation energies from the molecular orbital calculations can qualitatively be correlated with con-

* To whom correspondence should be addressed. E-mail: spgejji@chem.unipune.ernet.in. Fax: +91-20-25691728.

10.1021/jp054209g CCC: $33.50
Published on Web 12/14/2005

TABLE 1: Comparison of HF, B3LYP, and Experimental Vibrational Frequencies of TFSI, Diglyme, and Diglyme−LiTf

	B3LYP/6-31+G**	HF/6-31+G**	HF/6-31G**	Experimental
		TFSI		
SO stretch	1264 (359)	1330 (606)	1310 (737)	1354
	1251 (294)	1316 (433)	1285 (152)	1334
CS stretch	1176 (45)	1283 (87)	1261 (1)	
	1168 (199)	1282 (92)	1260 (328)	
CF stretch	1155 (156)	1257 (119)	1241 (297)	1240
	1148 (91)	1253 (127)	1235 (112)	
	1138 (236)	1243 (229)	1229 (444)	1227
	1133 (663)	1240 (680)	1227 (163)	
SN stretch	1077 (305)	1162 (631)	1132 (582)	1136
	1032 (221)	1145 (302)	1050 (11)	1060
	982 (441)	1079 (235)		
		Diglyme		
CH_2 scissor	1268 (19)	1499 (12)	1457 (12)	1453
	1463 (17)	1497 (10)	1454 (13)	
CH_2 rock		1474 (15)	1431 (21)	
	1379 (18)	1422 (34)	1381 (44)	1370
	1354 (69)	1398 (104)	1356 (122)	1354
CH_2 twist	1286 (69)	1319 (35)	1279 (32)	
	1243 (26)	1280 (42)	1241 (43)	
	1232 (13)	1268 (17)	1231 (18)	
		1248 (18)	1211 (161)	
CO stretch		1202 (52)		
CH_2 wag	1202 (44)	1194 (94)		
	1160 (29)	1184 (18)		
		1181 (65)		
CO stretch	1143 (110)	1172 (313)	1169 (51)	
	1124 (316)		1160 (88)	
			1148 (74)	
			1138 (393)	
CH_2 wag	1116 (49)	1152 (47)	1151 (19)	
			1121 (38)	
CC + CO stretch	1071 (15)	1105 (11)	1021 (37)	
	1020 (32)	959 (36)		
CH_2 wag	938 (32)	956 (15)	862 (42)	874
	859 (41)	885 (43)	839 (20)	855
	838 (17)	862 (19)		
		Diglyme−LiTf		
CH_2 scissor	1471 (20)	1499 (15)	1455 (14)	1460
	1467 (16)	1496 (14)	1453 (10)	
CH_2 rock	1379 (15)	1471 (10)	1379 (36)	1376
	1354 (35)	1420 (30)	1352 (77)	1352
		1394 (62)		
CH_2 twist	1246 (16)	1303 (18)	1265 (17)	
	1203 (33)	1280 (43)	1252 (24)	
		1266 (166)	1242 (45)	
		1266 (146)	1209 (79	
		1246 (50)	1157 (21	
		1239 (18)	1156 (41)	
CO stretch	1142 (44)	1194 (78)	1131 (507	
			1110 (253	
CH_2 wag	1132 (35)	1190 (89)	1064 (17)	
	1123 (283)	1158 (63)		
	1103 (28)			
CO stretch	1095 (188)	1163 (133)		
		1143 (261)		
CC + CO stretch	1055 (15)	1038 (73)	1010 (24	
	1009 (65)		1008 (61	
CH_2 wag	868 (29)	894 (27)	869 (37)	874
	839 (16)	858 (16)	825 (19)	836
	827 (13)	847 (17)		

ductivity data.[21] The Li−O interactions and the consequent vibrational spectra of crystalline phases of $P(EO)_6LiXF_6$ (X = P, As, and Sb) have been analyzed by Frech[22] et al. to understand the cation−polymer interactions in SPE. Ab initio HF calculations on the 1:1:1 ethylene glycol−M^+−X^- complexes have predicted that the bond distances in the SPE are shorter compared to those in free state.[23] It has been inferred that the metal ion binds stronger to the PEO oligomer than the counteranion in these electrolytes. As a pursuit of this in the present work, we investigate electronic structure and the normal vibration characteristics in the diglyme−M^+−X^- (M = Li, Na, and K and X = CF_3SO_3, PF_6, and $(CF_3SO_2)_2N$) electrolytes using the ab initio quantum chemical calculations. Normal vibrations have been assigned, and the frequency shifts of characteristics vibrations have been analyzed using the natural bond orbital (NBO) analysis and the molecular electron density (MED) topography. The computational method has been outlined in the following.

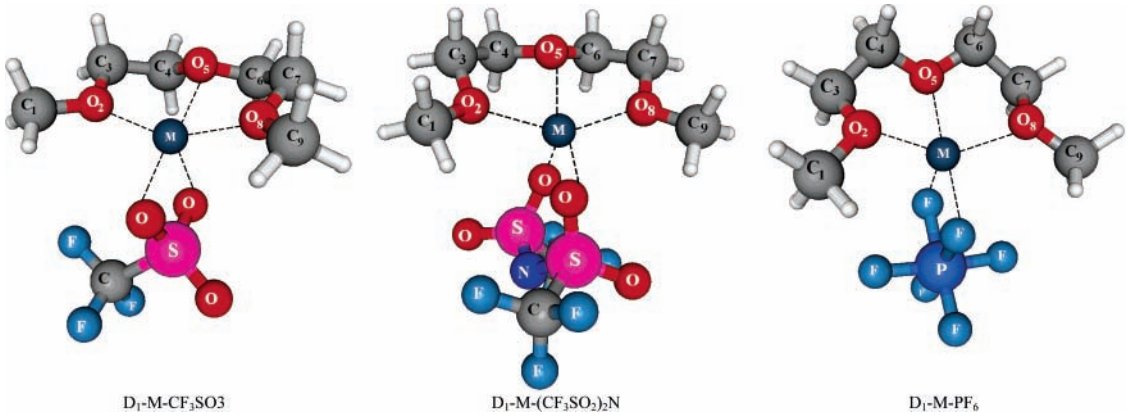

Figure 1. Optimized geometries of the $D_1-M^+X^-$ (M = Li, Na, and K and X = CF_3SO_3, PF_6, and $(CF_3SO_2)_2N$).

2. Computational Method

Geometry optimizations using the restricted Hartree−Fock (RHF) and the hybrid density functional theory incorporating Becke's three-parameter exchange with Lee, Yang, and Parr's (B3LYP) correlation functional[24,25] are performed on the $CH_3(OCH_2CH_2)_2OCH_3-M^+-X^-$ (M = Li, Na, and K and X = CF_3SO_3, $(CF_3SO_2)_2N$, and PF_6) systems using the GAUSSIAN03 program.[26] The internally stored 6-31G(d, p) and 6-31+G(d,p) basis sets were employed. Stationary point geometries obtained were characterized as the saddle points or local minima on the potential-energy surface by examining the number of imaginary frequencies and the eigenvalues of the Hessian matrix. Normal vibrations were assigned by visualizing displacements of atoms around their equilibrium (mean) positions.[27] Vibrational frequencies of diglyme−LiTf[28] and $TFSI^-$ anion[29] from the measured spectra are compared with those derived from the HF (using 6-31G(d,p) and the 6-31+G(d,p) basis sets) and the B3LYP/6-31(d,p) calculations (cf. Table 1). HF/6-31G** calculated (harmonic) vibrational frequencies scaled by 0.89 are reported in this table. This justifies the use of low-level HF/6-31G** calculations in the present work. NBO analysis was performed subsequently.[30] The MED topography[31] and the four types of nondegenerate critical points (CPs) of rank 3 have been identified in the three-dimensional space which include: (3, −3) maxima (e.g., nuclear position), (3, +3) minima generally known as cage critical points (ccp); saddle points denoted by (3, −1) and (3, +1), referred as the bond critical point (bcp) and ring critical point (rcp), respectively. The difference electron density ($\Delta\rho$) was calculated by subtracting the sum of electron densities of the alkali metal ion, diglyme, and the anion from the electron density of diglyme$-M^+-X^-$ (M = Li, Na, and K) (X = CF_3SO_3, PF_6, $(CF_3SO_2)_2N$). For obtaining the difference, electron density maps, diglyme, and corresponding anion geometries in 1:1:1 electrolytes were used. Thus difference electron density maps showing contours from ±0.001 to ±0.0009 au are displayed in Figure 2.

3. Results and Discussion

Optimized geometries of diglyme$-M^+-X^-$ (M = Li, Na, and K and X = Tf, PF_6, and TFSI) derived from the HF/6-31G(d,p) calculations are displayed in Figure 1 along with the atomic labels used. In the crystalline phase diglyme with all trans conformation around the C−O and C−C bonds is of minor importance.[32] We, therefore, consider diglyme possessing the gauche conformation around the C−C bonds of central CH_2-CH_2-O fragment as a reference in this work. Selected HF optimized geometrical parameters are reported in Table 2. The weakening of CO bonds engenders longer C_1-O_2 and C_8-O_9 bond distances compared to those in the gas-phase diglyme conformer. Bond angles generally are less sensitive to the metal ion interaction, and a largest deviation of 3° has been noticed for the COC bond angles. The interaction with a metal ion, however, brings about relatively large conformational change in the C−O−C backbone of PEO oligomer and accordingly a change of $C_3C_4O_5C_6$ and $C_6C_7O_8C_9$ dihedral angles from 180° (trans) to 72° (near gauche) has been noticed. (cf. Table 2).

For the electrolytes containing the triflate anion, the shortest Li−oxygen distance turns out to be 2.039 Å. On the other hand the SO bonds of the free lithium triflate ion pair has been predicted to be 1.471 Å. These bond distances in the electrolytes containing metal−triflate are shortened. Contraction of these bonds can qualitatively be correlated to the strength of metal−anion interactions. Thus shortening of SO* (O* denotes oxygen atom which binds to metal ion) bonds in LiTf−diglyme turns out to be 0.014 Å compared to 0.007 Å for NATf−diglyme and 0.003 Å for KTf−diglyme. It may, therefore, be inferred that neutral Li^+-Tf^- ion pairs are facilitated over Na^+-Tf^- or K^+-Tf^--containing electrolytes. Similar inferences can be drawn for electrolytes containing TFSI or PF_6^- anions.

For 1:1:1 SPE comprised of Tf^- anions, the alkali metal shows pentadentate coordination with the metal ion binding to three ether oxygens of diglyme and two oxygens of the Tf^- anion. This has also been observed in the crystal structure.[33−36] The cation size, however, is manifested in different binding modes of the alkali metal ion. Both TFSI- and PF_6-containing electrolytes yield hexadentate coordination for the metal ion in KTFSI, $NaPF_6$, and KPF_6 (cf. Figure 1). Bond angles of counteranion in these electrolytes are insensitive to such coordination.

Cation−polymer interactions in the crystals can be revealed from the spectroscopic analysis and studied extensively in the literature.[37,38] We compare the HF/6-31G(d,p) vibrational frequencies of diglyme−MX systems in the 820−1470-cm^{-1} region with the free diglyme in Table 3. As pointed out earlier, the cation−polymer interactions generally bring about a change in the conformation of the polymer backbone and consequent vibrational spectra. Assignment of these normal vibrations in the experimentally measured spectra in these SPE, however, is difficult. Theoretical calculated harmonic vibrational frequencies in this regard offer immense help in understanding the accompanying spectral changes. Alkali metal ion induced conformational change about the −O−C−C−O− framework of oligomer manifests in CH_2 rocking and C−O stretching vibrations.[39] Thus the 1431-cm^{-1} band (CH_2 rocking) of diglyme disappears in the infrared spectrum on cation coordination, and

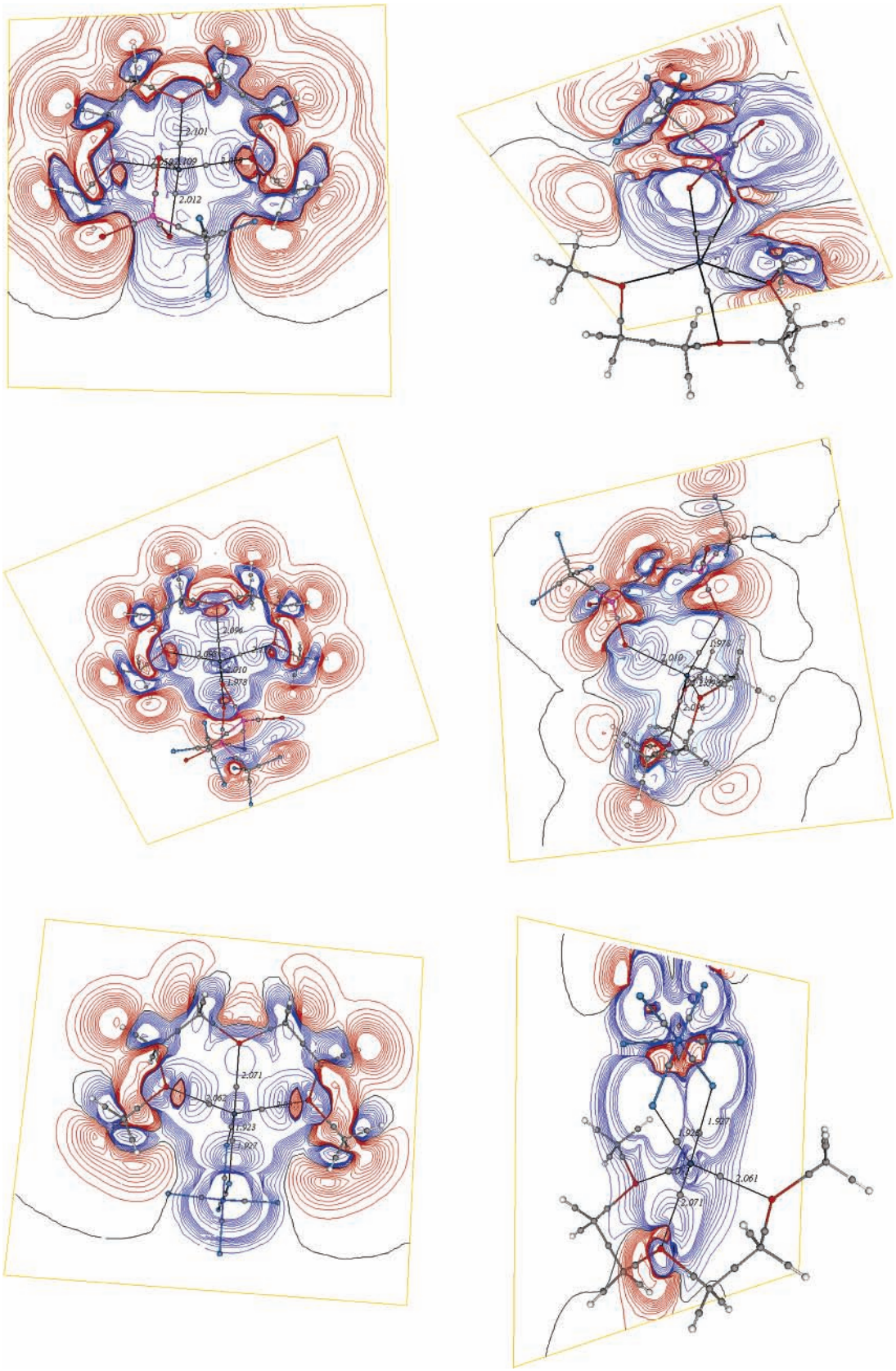

Figure 2. (a) Difference electron density maps in $D_1-Li-CF_3SO3$ (contours in the range of $\pm 0.001-0.0009$ au) are shown. Filled circles in black show the bond critical points. See text for details. The black line represents a zero valued contour. (b) Difference electron density maps in $D_1-Li-(CF_3SO_2)_2N$ (contours in the range of $\pm 0.001-0.0009$ au) are shown. Filled circles in black show the bond critical points. See text for details. Black line represents a zero valued contour. (c) Difference electron density maps in $D_1-Li-PF_6$ (contours in the range of $\pm 0.001-0.0009$ au) are shown. Filled circles in black show the bond critical points. See text for details. Black line represents a zero valued contour.

new 1105- and 1115-cm^{-1} vibrations appear instead. A downshift of 15 cm^{-1} has been predicted for the 1021-cm^{-1} vibration (CH_2 wag). An experimental infrared spectrum of the diglyme-lithium triflate[26] has also been reported in Table 3. As may

TABLE 2: Selected Optimized Geometrical Parameters (Bond lengths in Angstoms and Bond angles in Degrees) of Free Diglyme (D_1) and the $D_1-M^+X^-$ (M = Li, Na, and K and X = CF_3SO_3, PF_6, and $(CF_3SO_2)_2N$) Complexes

		$D_1-M-CF_3SO_3$			$D_1-M-(CF_3SO_2)_2N$			D_1-M-PF_6		
	D_1	Li	Na	K	Li	Na	K	Li	Na	K
C_1-O_2	1.391	1.405	1.409	1.408	1.405	1.410	1.407	1.413	1.411	1.411
O_2-C_3	1.392	1.401	1.400	1.397	1.400	1.399	1.397	1.403	1.398	1.396
C_3-C_4	1.510	1.514	1.511	1.511	1.512	1.511	1.511	1.511	1.510	1.511
C_4-O_5	1.393	1.404	1.401	1.401	1.405	1.402	1.402	1.403	1.404	1.404
O_5-C_6	1.393	1.405	1.403	1.401	1.404	1.403	1.401	1.403	1.402	1.400
C_6-C_7	1.510	1.514	1.511	1.511	1.512	1.511	1.511	1.511	1.510	1.510
C_7-O_8	1.392	1.400	1.399	1.397	1.399	1.400	1.398	1.403	1.400	1.400
O_8-C_9	1.391	1.406	1.411	1.408	1.407	1.411	1.406	1.413	1.410	1.405
O_2-M		2.039	2.367	2.771	2.113	2.378	2.777	2.063	2.394	3.568
O_5-M		2.101	2.367	2.856	2.096	2.365	2.856	2.072	2.381	2.826
O_8-M		2.059	2.387	2.771	2.098	2.376	2.785	2.066	2.393	2.805
$C_3-C_4-O_5$	109.4	106.2	108.2	109.1	106.4	108.2	109.3	107.2	108.4	109.3
$C_4-C_5-C_6$	114.5	117.5	115.9	115.1	117.0	115.9	114.8	116.8	108.5	114.8
$C_5-C_6-C_7$	109.4	106.2	108.2	109.1	106.4	108.2	109.3	107.2	115.3	109.3
$C_6-C_7-O_8$	109.4	107.3	108.4	109.3	107.5	108.4	109.4	107.3	108.5	109.6
$C_7-O_8-C_9$	114.3	115.8	114.4	114.3	115.1	114.5	114.2	114.5	108.5	113.9
$C_3-C_4-O_5-C_6$	−177.7	−52.6	−58.7	63.3	175.2	−174.9	64.0	54.0	59.7	178.2
$O_5-C_6-C_7-O_8$	−75.6	−171.3	−172.5	−176.9	−173.6	−173.8	−176.8	−163.4	174.4	−64.1
$C_6-C_7-O_8-C_9$	175.2	52.0	61.1	−63.3	53.6	60.4	−63.7	−54.2	−59.2	−175.8

TABLE 3: Selected HF Vibrational Frequencies of the $CH_3-(O-CH_2-CH_2-)_2O-CH_3M^+X^-$ (M = Li, Na, and K and X = CF_3SO_3, PF_6, and $(CF_3SO_2)_2N$)

	diglyme		diglyme−M− CF_3SO_3				diglyme−M−(C $F_3SO_2)_2N$			diglyme−M−PF_6		
			Li									
	expt.	HF	HF	expt.	Na	K	Li	Na	K	Li	Na	K
CH_2 scissor		1457 (12)	1455 (14)	1460	1455 (12)	1456 (13)	1455 (16)	1455 (15)	1456 (14)	1454 (14)	1450 (14)	1456 (13)
	1453	1454 (13)	1453 (10)		1454 (14)	1445 (11)	1453 (10)	1451 (15)	1447 (17)	1448 (25)	1446 (11)	1447 (11)
CH_2 rock		1431 (21)										
	1370	1381 (44)	1379 (36)	1376	1377 (32)	1382 (36)	1378 (37)	1379 (32)	1382 (30)	1377 (33)	1380 (34)	1382 (31)
	1354	1356 (122)	1352 (77)	1352	1352 (92)	1356 (95)	1352 (69)	1353 (83)	1355 (94)	1352 (70)	1354 (81)	1356 (90)
CH_2 twist		1279 (32)	1265 (17)		1270 (15)	1277 (32)	1264 (20)	1270 (26)	1275 (37)		1272 (18)	1278 (24)
					1259 (80)							
			1252 (24)		1259 (52)							
		1241 (43)	1242 (45)		1240 (50)	1243 (45)	1241 (38)	1241 (28)	1241 (48)	1242 (40)	1242 (40)	1240 (41)
		1231 (18)				1241 (96)						
						1230 (18)	1227 (17)					
						1219 (153)		1216 (116)				
		1211 (161)	1209 (79)		1205 (73)	1209 (97)	1210 (81)	1206 (94)	1210 (88)	1205 (65)	1208 (69)	1209 (67)
			1157 (21)		1156 (23)							
			1156 (41)									
CO stretch		1169 (51)										
		1160 (88)					1158 (67)	1157 (36)		1158 (117)		
					1155 (52)	1155 (34)		1154 (35)	1155 (44)		1153 (52)	
			1131 (507)		1125 (151)	1132 (211)			1131 (198)			1129 (196)
			1110 (253)									
CH_2 wag		1151 (19)	1064 (17)				1157 (49)	1126 (148)		1128 (29)	1125 (114)	
CO stretch		1148 (74)										
		1138 (393)					1129 (177)				1122 (175)	
CH_2 wag		1121 (38)			1121 (127)	1118 (37)		1121 (152)	1116 (69)			1117 (58)
										1090 (76)		
CO stretch					1105 (261)	1112 (368)	1111 (266)	1105 (266)	1112 (256)	1115 (310)	1104 (319)	1110 (353)
CC + CO stretch		1021 (37)	1010 (24)		1010 (62)	1011 (53)	1008 (76)	1012 (20)	1011 (66)	1004 (89)	1008 (82)	1010 (72)
CH_2 wag	874	862 (42)	869 (37)	874	858 (37)	862 (46)	870 (27)	858 (31)	862 (41)	861 (120)	859 (77)	861 (76)
	855	839 (20)	825 (19)	836	827 (19)	829 (19)	823 (19)	827 (18)	827 (21)	830 (17)	828 (16)	828 (19)

readily be noticed, the 1489-cm^{-1} band in diglyme downshifts to 1476 cm^{-1} on interaction with the $LiCF_3SO_3$, and a doublet separated by 16 cm^{-1} (~1370 and 1354 cm^{-1}) has been observed in the infrared spectrum of diglyme. HF calculations predict a near doublet assigned to the CH_2 rock vibrations at 1381 and 1356 cm^{-1} ($\Delta\upsilon = 15$ cm^{-1}) in the diglyme conformer. This separation increases to 27 cm^{-1} in the electrolytes containing $LiCF_3SO_3$, which has also been observed in the experiment. Similar inferences can be drawn for the electrolytes containing other alkali metal triflates. The cation ether oxygen interactions engender a downshift of 19 cm^{-1} for the 855-cm^{-1} vibration in observed infrared spectrum of diglyme and corresponds to the 839-cm^{-1} vibration. The latter has been downshifted to 825 cm^{-1}. It should be remarked that the vibrations of the atoms not interacting with the metal ion lead to frequency shifts in the opposite direction and engender blue shift in the infrared spectrum.

Theoretical vibrational frequencies in the region 845−1290 cm^{-1} of the free anions and in the 1:1:1 electrolytes are displayed in Table 4. It may be inferred that weakening of bonds participating in the metal−anion interactions lead to red shift of the X−Y (X = O and F and Y = P and S) vibrations compared to those in the free anions. Accordingly a large red shift of 102 cm^{-1} for the S−O* stretching vibration (O* denotes

TABLE 4: Bond Length, Vibrational Frequency, and Electron Density in Antibonding Orbitals

	M−Tf−Diglyme (M = Li, Na, and K)											
	CF_3SO_3–			D1−Li−CF_3SO_3			D_1−NaCF_3SO_3			D_1−KCF_3SO_3		
	Å	n	r	Å	n	r	Å	n	r	Å	n	r
SO*	1.443	1244(5 68)	0.136	1.463	1283 (506)	0.142	1.458	1279 (445)	0.141	1.455	1285 (454)	0.142
SO*	1.443		0.136	1.457	1153 (277)	0.139	1.457	1162(2 17)	0.140	1.455	1174 (254)	0.141
SO	1.443		0.136	1.426		0.123	1.428		0.125	1.427		0.124
CF	1.323	1195 (78)	0.081	1.312	1250 (338)	0.079	1.312	1251 (366)	0.078	1.313	1249 (407)	0.078
CF	1.323		0.081	1.319	1223 (120)	0.083	1.322	1216 (116)	0.084	1.329	1194 (172)	0.086
CF	1.323		0.081	1.312		0.079	1.312		0.078	1.313		0.078
MO				2.012			2.321			2.700		
MO				2.109			2.340			2.700		
MO												

	M−TFSI−Diglyme (M = Li, Na, and K)											
	$(CF_3SO_2)_2N^-$			D_1−Li−$(CF_3SO_2)_2N$			D_1−Na−$(CF_3SO_2)_2N$			D_1−K−$(CF_3SO_2)_2N$		
	Å	n	r	Å	n	r	Å	n	r	Å	n	r
SO*	1.431	1310 (737)	0.123	1.454	1294 (677)	0.134	1.450	1289 (718)	0.108	1.447	1299 (668)	0.131
SO	1.430	1285 (152)	0.113	1.422		0.106	1.424		0.133	1.421		0.108
SO	1.430		0.113	1.427		0.118	1.429		0.131	1.443		0.126
SO*	1.431		0.123	1.450		0.133	1.450		0.120	1.443		0.126
CF	1.313	1241 (297)	0.080	1.312	1283 (612)	0.081	1.312	1283 (608)	0.081	1.314	1279 (385)	0.083
CF	1.314	1235 (112)	0.080	1.311	1267 (390)	0.081	1.311	1265 (262)	0.080	1.313	1263 (170)	0.079
CF	1.318	1229 (444)	0.080	1.309		0.080	1.310	1260 (82)	0.079	1.312	1261 (222)	0.079
CF	1.313		0.080	1.309		0.078	1.307		0.078	1.307		0.078
CF	1.314		0.080	1.306		0.078	1.307		0.078	1.306		0.078
CF	1.318		0.080	1.304		0.078	1.305		0.078	1.305		0.078
M−O				1.978			2.272			2.708		
M−O				2.010			2.287			2.899		
M−O										2.901		

	M−PF_6−Diglyme (M = Li, Na, and K)											
	PF_6^-			D1−Li−PF_6			D_1−Na−PF_6			D_1−K−PF_6		
	Å	n	r	Å	n	r	Å	n	r	Å	n	r
PF*	1.606	882(47 6)	0.098	1.662	908 (407)	0.108	1.642	887 (440)	0.105	1.635	887 (453)	0.104
PF*	1.606		0.098	1.655	883 (397)	0.107	1.637	886 (423)	0.104	1.633	885 (456)	0.103
PF*	1.606		0.098	1.592	861 (120)	0.096	1.634	886 (423)	0.104	1.631	884 (417)	0.103
PF	1.606		0.098	1.591		0.096	1.579		0.094	1.583		0.095
PF	1.606		0.098	2.574		0.093	1.577		0.094	1.580		0.094
PF	1.606		0.098	1.574		0.093	1.576		0.094	1.580		0.094
M−O				1.923			2.286			2.657		
M−O				1.927			2.319			2.667		
M−O							2.374			2.668		

oxygens interacting with the metal ion) has been predicted for the $CH_3(OCH_2CH_2)_2OCH_3$−Li−CF_3SO_3 electrolytes compared to the 1398-cm^{-1} vibration of the free triflate anion. On the other hand reorganization of electron distribution due to anion−alkali metal ion interactions cause a shift in the opposite direction for the vibrations involving atoms which do not participate in these interactions.[40] Accordingly the free SO (for oxygen atoms not participating in the interactions) and CF stretchings engender a blue shift of ∼40 and 60 cm^{-1}, respectively, in $CH_3(OCH_2CH_2)_2OCH_3$−Li−CF_3SO_3 electrolytes. The $\nu_s(SO_3)$ and $\delta_s(CF_3)$ stretching vibrations in these SPE are dependent on the alkali metal ion and stems from the different potential energy environmental of the $CF_3SO_3^-$. The inferences thus obtained agree well with the observed infrared or Raman spectra.[38]

Spectroscopic characterization of the conformational states of the $TFSI^-$ has been studied experimentally.[29] The SO_2 stretchings appears as a doublet at ∼1354 cm^{-1} and 1333 cm^{-1} and a locally symmetric vibration at 1136 cm^{-1}. A near doublet at 1310 and 1285 cm^{-1} of intense bands, with a separation of 25 cm^{-1}, has been predicted from the present calculations. The 1136-cm^{-1} band, however, was difficult to correlate with any of the vibrations obtained from the theoretical calculations. CF stretching assigned to the 1240-cm^{-1} band agrees well with those calculated from theoretical calculations. The measured infrared spectra by Doeff[41] have shown that with increasing salt concentration the $\delta_s(CF_3)$ bands shifts to higher wavenumber, which has been attributed to stronger cation−anion interactions with increase in salt concentration. The present calculations have shown that for the LiTFSI-containing electrolytes 1241 cm^{-1} vibration of the free TFSI anion moves to 1283 cm^{-1}. This vibration has been assigned to the CF stretching and is comprised of the fluorines, which do not participate in the cation−anion interactions.

Frech et al have measured the infrared and Raman spectra of the $CH_3(OCH_2CH_2)_2OCH_3$−Li−XF_6 (X = P, As, and Sb). These authors have pointed out that the vibration frequencies in these electrolytes depend on the Li−X distances. As seen from our calculations for the $LiPF_6$ complexed with the $CH_3(OCH_2CH_2)_2OCH_3$ a blue shift of 29 cm^{-1} for the 882-cm^{-1} vibration has been predicted. These blue shifts in electrolytes containing MPF_6 can be analyzed by studying the M−F (M = Li, Na, K) interactions. A largest blue shift is predicted for the $LiPF_6$. These frequency shifts to either higher or lower wavenumber can partly be attributed to oxygen−metal and metal−anion interactions as discussed in ref 19.

As may be inferred, the oligomer−metal ion and the metal ion−anion interaction bring about variation of strengths of bonds in the anion in SPE. In the following we investigate such bond strength variation utilizing the NBO analysis. Thus electron density in the antibonding orbital of various bonds of $CF_3SO_3^-$, $(CF_3SO_2)_2N^-$, and PF_6^- anions in their free state and in the

TABLE 5: Electron Densities at the bcps of Different Bonds in M−Tf−Diglyme, M−TFSI−Diglyme, and M−PF6−Diglyme (M = Li, Na, and K)

	M−Tf−Diglyme			
	$CF_3SO_3^-$	$D_1-Li-CF_3SO_3$	$D_1-NaCF_3SO_3$	$D_1-KCF_3SO_3$
	ρ_{bcp}	ρ_{bcp}	ρ_{bcp}	ρ_{bcp}
SO*	0.29774	0.28757	0.28973	0.29037
SO*	0.29774	0.29403	0.29046	0.29037
SO	0.29774	0.30697	0.30582	0.30633
CF	0.27561	0.28738	0.28743	0.27151
CF	0.27561	0.28093	0.27821	0.28549
CF	0.27561	0.28757	0.28730	0.28549
MO		0.02334	0.01994	0.01849
MO		0.01800	0.02100	0.01850
	M−TFSI−Diglyme			
	$(CF_3SO_2)_2N^-$	$D_1-Li-(CF_3SO_2)_2N$	$D_1-Na-(CF_3SO_2)_2N$	$D_1-K-(CF_3SO_2)_2N$
	ρ_{bcp}	ρ_{bcp}	ρ_{bcp}	ρ_{bcp}
SO*	0.304	0.29044	0.29153	0.29775
SO*	0.304	0.29143	0.30885	0.29775
SO	0.305	0.30711	0.30570	0.29362
SO	0.305	0.3100	0.29273	0.30999
CF	0.28153	0.28824	0.28862	0.28599
CF	0.28253	0.28974	0.28908	0.28779
CF	0.28506	0.29020	0.29020	0.28794
CF	0.28507	0.29063	0.29230	0.29363
CF	0.28631	0.29333	0.29302	0.29470
CF	0.28632	0.29530	0.29434	0.29363
M−O		0.02292	0.02111	0.01610
M−O		0.02063	0.02079	0.01172
M−O				0.01166
	M−PF_6−Diglyme			
	Pf_6^-	$D_1-Li-Pf_6$	$D_1-Na-Pf_6$	D_1-K-Pf_6
	ρ_{bcp}	ρ_{bcp}	ρ_{bcp}	ρ_{bcp}
PF*	0.14707	0.12704	0.13444	0.13745
PF*	0.14707	0.12963	0.13601	0.13659
PF*	0.14707	0.15340	0.13730	0.13791
PF	0.14707	0.15343	0.15795	0.15650
PF	0.14707	0.15967	0.15882	0.15757
PF	0.14707	0.15989	0.15893	0.15776
M−O		0.02357	0.01854	0.01618
M−O		0.02353	0.01685	0.01607
M−O			0.01456	0.01598
M−O				

1:1:1 SPE are summarized in Table 4. The anion−cation interactions result in an increase of electron density in the localized antibonding orbital of the anion, which results from a charge transfer to the alkali metal and leads to weakening of the bond. In other words an increase of electron density in the antibonding orbital of the bond participating in such anion−metal (Li, Na, and K) interactions leads to the bond elongation and consequently a red shift of stretching vibration compared to the corresponding vibration in the infrared spectrum of the free anion. On the other hand the electron density redistribution cause a transfer of a larger portion of electron density to the noninteracting bonds of the anion in these SPE which increase the bond strength causing bond contraction and hence a frequency upshift for the corresponding vibration. The blue shifts of the CF and SO stretching vibrations in the TFSI and triflate anion containing SPE can be explained. The vibrational frequency shifts in the $LiPF_6$ containing SPE can also be explained by using similar arguments.

We now discuss how the MED critical point (cf. section 2) topography can be utilized to understand the direction of frequency shifts caused by the anion−cation interactions. Electron density at the bond critical point (ρ_{bcp}) in these anions in free state and in the 1:1:1 electrolytes are reported in Table 5. The ρ_{bcp} values give a measure of strength of interaction.[42−43] Thus it may be conjectured that ρ_{bcp} emerge as a signature of the metal ether oxygen atoms or metal anion interactions. These electron densities at the bcp in the MED topography are in the range of 0.002−0.035 au. The red shifts of stretching vibrations are in accordance with the ρ_{bcp} values (cf. Table 5). Conversely blue shifts for frequencies of normal vibrations can be rationalized.

In the following we discuss how the difference electron density can be utilized to study the reorganization of electron density due to the metal ion−oligomer and cation−anion interactions in SPE. The difference electron density, $\Delta\rho$, was calculated by subtracting the sum of electron densities of the individual anion, cation, and diglyme from the corresponding electron density of the $CH_3(OCH_2CH_2)_2OCH_3-Li^+-X^-$ (X = CF_3SO_3, PF_6, $(CF_3SO_2)_2N$). Figure 2 displays the difference electron density maps for the Li^+-X^--containing SPE as an illustrative example. Difference electron density maps of the these SPE-containing Li^+ with $(CF_3SO_2)_2N^-$, $CF_3SO_3^-$, and PF_6^- counteranions are shown in parts a−c of Figure 2. To explain the direction of the frequency shifts of characteristics vibrations of diglyme and those of the counteranion, we derive the difference electron density contours in (i) a plane passing through the ether oxygens of diglyme in these electrolytes and (ii) a plane passing through all the atoms of the counter-anion present in the anion−metal interactions. The $\Delta\rho$ contours in the range of ±0.001−0.0009 au are displayed in Figure 2 where the blue lines represent positive valued contours and the negative valued contours appear in red. The zero-valued contour is

depicted as a black line. Figure 2a shows the difference electron density of the electrolyte comprised of diglyme complexed with the $Li(CF_3SO_2)_2N$. As may be noticed, the bcp of the C−O−C bonds wherein oxygen atoms participate in the O···Li interactions appear in a region (red) where the electron density is depleted. This explains a "red shift" of the C−O−C stretching vibration of diglyme in the above electrolyte compared to the corresponding vibration in the diglyme conformer. In contrast for the C−C and C−H bonds of diglyme, the bcp emerges in the (blue) region where the electron density is enhanced. This leads to increase of bond strength and hence a shift to higher wavenumber. As far as anionic vibrations in these SPE the bcp of CF bonds appear in a blue region (bond strengthening) in contrast to the SO bonds of the anion for which the bcp has been located in red region when oxygens coordinate to the metal ion. For the remaining SO bonds, the bcp has been identified in a blue region and, therefore, causes an "upshift" in frequency for the corresponding stretching. Thus the direction of frequency shifts of different anionic SO_2 and CF_3 stretching vibrations in the SPE containing TFSI anion can be explained.

Difference electron density contours for the electrolytes comprised of diglyme complexed with LiTf have been depicted in Figure 2b. As explained earlier, the bond critical point of the blue-shifted CF bond lies in a region (blue contours) where the electron density is increased, whereas for the red-shifted SO bond the bcp appear in region with decreased electron density (red contours).

In Figure 2c, the difference electron density for electrolytes containing diglyme−$LiPF_6$ are shown. As inferred earlier the distinction of the direction frequency shifts has been facilitated through whether the bcp appears in blue or red contour(s) regions. Here again the fluorine atoms not interacting with a metal ion engender frequency upshift for the PF stretching and can be distinguished from the rest. It should be remarked here that the direction of the frequency shifts of characteristics vibrations in the electrolytes containing Na^+ or K^+ ions can also be rationalized from the difference electron density maps.

4. Conclusions

Systematic investigations of structural and vibrational spectra of $CH_3(OCH_2CH_2)_2OCH_3M^+X^-$ (M = Li, Na, and K and X = CF_3SO_3, PF_6, and $(CF_3SO_2)_2N$) in the 1:1:1 polymer electrolytes have been presented. The conclusions of this work are summarized as follows. (i) In the electrolytes comprised of alkali metal triflates, the metal ion is in pentadentate coordination, via three ether oxygens of diglyme and two from the anion. X-ray crystal structure of LiTf complexed with diglyme is in a good agreement with that obtained from the present calculations. For the electrolytes containing PF_6 binding of Na^+ and K^+, however, is qualitatively different from that of lithium. In these electrolytes the Na^+ and K^+ ions interact with three fluorine atoms of the anion and three oxygens of the diglyme. In case of electrolytes containing TFSI anion large size of K^+ facilities binding to three oxygens from different SO_2 groups of the anion and is qualitatively different from those for Li^+ or Na^+. In the latter bidentate coordination with oxygen from each SO_2 groups of the anion has been predicted. (ii) From the metal ion and ether oxygen distances in these SPE it has been suggested that 1:1 diglyme−cation ion pairs are favored in electrolytes containing Li^+ than those comprised of Na^+ or K^+. (iii) Conformational change around the C−O bonds of diglyme−MX systems engenders a change in the vibrational spectra. Consequently the 1431-cm^{-1} vibration of free diglyme (assigned to CH_2 rocking) vanishes in the 1:1:1 electrolytes. A downshift of C−O−C stretching vibration correlates with the strength of metal−ether oxygen interactions. A near doublet at 1370 and 1354 cm^{-1} in the observed infrared spectrum of diglyme conformer gets more separated in the LiTf-containing electrolytes. This agrees well with the HF/6-31G(d,p) calculations, wherein 1381- and 1356-cm^{-1} vibrations of the diglyme conformer get more separated (nearly twice as large) in the 1:1:1 electrolytes. (iv) Contraction of the CF bonds of the anion in the electrolytes containing $LiCF_3SO_3$ or $Li(CF_3SO_2)_2N$ engenders a blue shift of 62 and 42 cm^{-1} for the stretching vibrations, respectively. The 889-cm^{-1} stretching of the free PF_6 upshifts to 918 cm^{-1} in diglyme−$LiPF_6$ containing electrolytes. (v) The direction of frequency shifts due to the metal−ether oxygen and metal−anion molecular interactions can be explained from the NBO analysis. Analogously increase in the strengths of the CF bonds in Tf^- or $TFSI^-$anions in SPE can be explained from the MED topography. Thus the difference electron density maps can be utilized to understand the direction of frequency shifts of the "anionic vibrations" in these electrolytes. These conclusions are supported by the NBO analysis.

Acknowledgment. S.P.G. acknowledges the support from the Council of Scientific and Industrial Research (Project 01-(1772)/02/EMR-II), New Delhi, India.

References and Notes

(1) Chatani, Y.; Fujii, Y.; Takayanagi, T.; Honma, A. *Polymer* **1990**, *31*, 2238.
(2) Wright, P. V. *Br. Polym.* **1975**, *7*, 319.
(3) Wright, P. V. *Polym. Phys. Edn.* **1976**, *14*, 955.
(4) Chatani, Y.; Okamura, S. *Polymer* **1987**, *28*, 1815.
(5) Lauenstein, A.; Tegenfeldt, J. *J. Phys. Chem. B* **1998**, *102*, 6702.
(6) Johansson, P. *Polymer* **2003**, *48*, 2291.
(7) Johansson, P.; Jacobsson, P. *J. Phys. Chem. A.* **2001**, *105*, 8504.
(8) Johansson, P.; Gejji, S. P.; Tegenfeldt, J.; Lindgren, J. *Solid State Ionics* **1996**, *86*−*88*, 297.
(9) Baboul, A. G.; Redfern, P. C.; Sutjianto, A.; Curtiss, L. A. *J. Am. Chem. Soc.* **1999**, *121*, 7220.
(10) Gejji, S. P.; Johansson, P.; Tegenfeldt, J.; Lindgren, J. *Comput. Polym Sci.* **1995**, 5, 99.
(11) Johansson, P.; Tegenfeldt, J.; Lindgren, J. *Polymer* **2001**, *42*, 6573.
(12) Gejji, S. P.; Hermansson, K.; Lindgren, J. *J. Phys. Chem. A.* **1993**, *97*, 3712.
(13) Gejji, S. P.; Hermansson, K.; Tegenfeldt, J. Lindgren, J. *J. Phys. Chem. A.* **1993**, *97*, 11402.
(14) Frech, R.; Rhodes, C. P.; Khan, M. *Macromol. Symp.* **2002**.
(15) Rhodes, C. P.; Khan, M.; Frech, R. *J. Phys. Chem. B.* **2002**, *106*, 10330.
(16) Rodes, C. P.; Frech, R. *Macromolecules* **2001**, *34*, 1365.
(17) Frech, R.; Seneviratne, V.; Gadjourova, Z. Bruce, P. *J. Phys. Chem. B.* **2003**, *107*, 11255.
(18) Johnston, D. H.; Shriver, D. F. *Inorg. Chem.* **1993**, *32*, 1045.
(19) Huang, W.; Frech, R.; Wheeler, R. A. *J. Phys. Chem.* **1994**, *98*, 100.
(20) Burba, C. M. Frech, R. *60th Southwest regional Meeting of the American Chemical Society*; Forth Worth, TX, September 29, 2004.
(21) Johansson, P.; Jacobsson, P.*Electrochim. Acta* **2003**, *48*, 2279.
(22) Bruce, P. G.; Gray, F. M. *Solid State Electrochemistry*; Cambridge: New York, 1995; p 119.
(23) Johansson, P.; Jacobsson, P. *J. Phys. Chem. A.* **2001**, *105*, 8504.
(24) Becke, D. *J Chem. Phys.* **1993**, *98*, 5684.
(25) Lee, C.; Yang, W.; Parr, R. G. *Phys. Rev.* **1988**, *B37*, 785.
(26) Frisch, M. J.; Trucks, G. W.; Schlegel, H. B.; Scuseria, G. E.; Robb, M. A.; Cheeseman, J. R.; Montgomery, J. A.; Vreven, Jr. T.; Kudin, K. N.; Burant, J. C.; Millam, J. M.; Iyengar, S. S.; Tomasi, J.; Barone, V.; Mennucci, B.; Cossi, M.; Scalmani, G.; Rega, N.; Petersson, G. A.; Nakatsuji, H.; Hada, M.; Ehara, M.; Toyota, K.; Fukuda, R.; Hasegawa, J.; Ishida, M.; Nakajima, T.; Honda, Y.; Kitao, O.; Nakai, H.; Klene, M.; Li, X.; Knox, J. E.; Hratchian, H. P.; Cross, J. B.; Adamo, C.; Jaramillo, J.; Gomperts, R.; Stratmann, R. E.; Yazyev, O.; Austin, A. J.; Cammi, R.; Pomelli, C.; Ochterski, J. W.; Ayala, P. Y.; Morokuma, K.; Voth, G. A.; Salvador, P.; Dannenberg, J. J.; Zakrzewski, V. G.; Dapprich, S.; Daniels, A. D.; Strain, M. C.; Farkas, O.; Malick, D. K.; Rabuck, A. D.; Raghavachari, K.; Foresman, J. B.; Ortiz, J. V.; Cui, Q.; Baboul, A. G.; Clifford, S.; Cioslowski, J.; Stefanov, B. B.; Liu, G.; Liashenko, A.; Piskorz, P.; Komaromi, I.; Martin, R. L.; Fox, D. J.; Keith, T.; Al-Laham, M. A.; Peng, C. Y.; Nanayakkara, A.; Challacombe, M.; Gill, P. M. W.; Johnson,

B.; Chen, W.; Wong, M. W. Gonzalez, C.; Pople, J. A. *Gaussion 03*; Gaussian, Inc., Wallingford CT, 2004
(27) Limaye, A. C.; Gadre, S. R. *Curr. Sci.* **2001**, *80*, 1298.
(28) Frech, R.; Huang, W. *Macromolecules* **1995**, *28*, 1246.
(29) Herstedt, M.; Smirnov, M.; Johansson, P.; Chami, M.; Grondin, J.; Servant, J.; Lassegues, J. C. *J. Raman Spectrosc.* In press.
(30) Reed, A. E.; Curtiss, L. A.; Weinhold, F. *Chem. Rev.* **1988**, *88*, 899.
(31) Balanarayan, P.: Gadre, S. R. *J. Chem. Phys.* **2003**, *119*, 5037.
(32) Kearley, G. J.; Johansson, P.; Delaplane, R. G.; Lindgren, J. *Solid State Ionics* **2002**, *147*, 237.
(33) Frech, R.; Seneviratne, V. *Abstracts, 59th SouthWest Regional Meeting of the American Chemical Society* October 25−28, **2003**.
(34) Frech, R.; Rhodes, C. P.; Khan, M. *Macromol. Symp.* **2002**.
(35) Rhodes, C. P.; Frech, R. *Macromolecules* **2001**, *34*, 2660.
(36) Henderson, W. A.; Young, V. G.; Brooks, N. R.; Smyrl, W. H. *Acta Crystallogr., Sect. C* **2002**, *C58*, 201.
(37) Chintapalli, S.; Frech, R. *Electrochim. Acta* **1995**, *40*, 2093.
(38) Rhodes, C. P.; Frech, R. *Solid State Ionics* **2002**, *136*, 1131.
(39) Frech, R.; Chintapalli, S. Bruce, P. G. Vincent, C. A. *Macromolecules* **1999**, *32*, 808.
(40) Hobza, P.; Havlas, Z. *Chem. Rev.* **2000**, *100*, 4253.
(41) Ferry, A.; Doeff, M. M.; De Jonghe, L. C. *J. Electrochem. Soc.* **1998**, *145*, 1586.
(42) Kock, U.; Popelier, P. L. A. *J. Phys Chem. A* **1995**, *99*, 9747.
(43) Popelier, P. L. A. *J. Phys. Chem. A.* **1998**, *102*, 1873.